Surface and Coatings Technology, Volume 204, Issue 15, 25 April 2010, Pages 2331-2336


# Accepted Manuscript

Nickel Titanium and Nickel Titanium Hafnium Shape Memory Alloy thin films

J. Rao, T. Roberts, K. Lawson, J. Nicholls

PII: S0257-8972(10)00003-4
DOI: doi: 10.1016/j.surfcoat.2009.12.025
Reference: SCT 15461

To appear in: *Surface & Coatings Technology*

Received date: 25 February 2009
Accepted date: 29 December 2009

Please cite this article as: J. Rao, T. Roberts, K. Lawson, J. Nicholls, Nickel Titanium and Nickel Titanium Hafnium Shape Memory Alloy thin films, *Surface & Coatings Technology* (2010), doi: 10.1016/j.surfcoat.2009.12.025

# Nickel Titanium and Nickel Titanium Hafnium Shape Memory Alloy thin films.

**J.Rao*, T. Roberts, K. Lawson, J. Nicholls**

School of Applied Science, Cranfield University, Bedfordshire, MK43 0AL.

## Abstract

Shape Memory Alloys (SMAs) coatings of NiTi and NiTiHf have been deposited onto Si substrates using pulse DC sputtering. Coatings of NiTi with compositions containing 45 to 65 at% Ti have been fabricated by co-sputtering NiTi with Ti. NiTiHf coatings with Hf compositions ranging from 2 to 30 at% Hf have been fabricated by co-sputtering NiTi with Hf. XRD results reveal the as-deposited coatings are amorphous. A high temperature, 1100$^{o}$C anneal followed by a low temperature, 550$^{o}$C anneal was employed to crystallise the coatings. The XRD then shows the coatings to be martensitic at room temperature.

Two sets of samples were produced for characterisation; one set was used for indentation studies and the other set used to prepare freestanding films required for differential scanning calorimetry, (DSC) studies.

Using the DSC, a NiTi coating containing 52 at% Ti shows an endothermic austenite peak phase transformation, ($A_p$) at around 105$^{o}$C and an exothermic peak martensite phase transformation, ($M_p$) at 65$^{o}$C, resulting in a hysteresis of 40$^{o}$C. For a NiTi coating containing 65 at% Ti the hysteresis remained unchanged at 40$^{o}$C, but there was a decrease in the phase transformation enthalpies when compared with the coatings containing 52 at% Ti. Calculated phase transformation enthalpies in the NiTi coatings ranged from 6 to 13 J/g for the austenite phase and -8 to -11 J/g for the martensite phase.

* Corresponding author: Tel: + 44 1234 750111, Fax: +44 1234 752473, email: j.rao@cranfield.ac.uk

The NiTiHf coating shows SMA behaviour for a film containing 30 at% Hf. DSC reveals an 'R' phase transition in this film. It is understood that this phase is present in films that have high internal stresses and is understood to nucleate near $Ti_3Ni_4$ precipitates. Phase transformation temperatures occur at 98$^o$C and 149$^o$C during heating and occur at 99$^o$C during cooling. Phase transformation enthalpies range between 2 and 3 J/g for the austenite phase and -7 J/g for the martensite phase.

A scratch tester equipped with a 5mm spherical tip has been utilised with loads ranging from 1 to 5N to determine the recovery properties of the films. The results in this study conclude that NiTi films containing 65 at% Ti deform 3 times more than films containing 52 at% Ti. For NiTiHf thin films, increasing the Hf composition from 2 at% to 30 at%, doubled the deformation measured in the coatings.

*Keywords. SMA, NiTi, NiTiHf, Sputtering, Thin Films.*

PCAS Codes: 50, 60 and 70.

# 1.0 Introduction

NiTi is an intermetallic alloy that has demonstrated a unique ability to recover its original shape after deformation. The application of heat or applied stress allows the recovery of the intermetallic alloy through a reversible thermo-elastic phase transformation without long-range diffusion or a change in composition. NiTi can transform from a low temperature, low allotrope martensite B19' phase to a high temperature, high-symmetry allotrope austenite B2 phase, upon the application of heat or applied stress. There is very little volume change in the transformations, but the lattice change between the high temperature body-centered cubic phase and the low temperature, ordered monoclinic phase involves a large local shear strain. In NiTi, this phase transformation takes place at temperatures below 373K and has generated a number of studies on NiTi shape memory alloy (SMA) thin films in an array of novel applications ranging from medical applications[1] to micro-actuators [2-4]. However, as the phase transformation temperatures are below 373K [5,6], the range of applications where NiTi could be applied is limited to below this temperature.

There are another group of ternary SMA materials in the NiTiX group, where X are substitutional solutions of Hf, Zr, Au, Pd or Pt, which have aroused interest as future SMAs materials that have phase transformation temperatures that are greater than 373K [7], and therefore could be utilised in high temperature micro actuator applications such as those experienced in a gas turbine [8]. Substitutions of an additional element of Hf [9], Pd [10] and Pt [11] have proved effective at increasing phase transformation temperatures above 773K [12]. However, the material costs associated, in particular, with the inclusion of Pt and Pd metals have limited applications to niche markets [10]. The addition of Hf in a NiTiX material system has been particularly important as an alternative high-temperature SMA because of its

low cost, its performance at modest doping levels [7]and high transformation temperatures [12,13], opening up the possibility of a wider range of high temperature applications. The NiTiHf material system has an additional advantage of being more stable than NiTi during thermal cycling and stable during high temperature aging [7].

The underlying process route for the deposition of SMA materials as a coating has been either RF [14]or conventional DC sputtering [12]. Recent advances in pulse DC sputtering have proven to produce greater plasma densities [15,16] leading to higher ionisation of the sputtered materials. The resulting films produced are denser than those films produced by conventional sputtering routes [17].

The complex behaviour of SMAs show that they are very sensitive to an array of physical factors such as alloy composition, lattice defects, microstructure and intrinsic stresses [7]. Pulse DC sputtering thus offers an opportunity to overcome and deposit SMA coatings that minimise the effects of defects, stress and other microstructural effects that impact SMA phase transformation. In fact it has been determined that there are stark differences in the response of stress-strain behaviour caused by internal stress due to $Ti_3Ni_4$ precipitates [18].

The aim of this study is to co-sputter NiTi, Ti and Hf using pulse DC sputtering and characterise the resulting NiTi and NiTiHf coatings. An understanding and the control of the film composition and its impact on phase transformations is a critical first step. The coatings are characterised for their phase transformation properties using a differential scanning calorimeter, (DSC), and their physical recovery properties interrogated with a 1 to 5 N load applied using a conventional scratch tester.

## 2.0 Experimental

All research work is undertaken in a Leybold L560® coater equipped with two 3-inch (75mm) magnetrons. The system is turbo-pumped to base pressure better than $10^{-7}$

Torr. The NiTi target is supplied by Teer Coatings [19] and is a NiTi intermetallic alloy of 50:50 at% (55:45 NiTi wt%). The Hf target is provided by Pi-Kem [20] with a quoted purity of 99.95%. Silicon (100) wafers are used as substrates in this study. All coatings were deposited at room temperature. For deposition, argon is used as the process gas at a pressure of 10mTorr and the target-substrate distance is kept constant at 7cm. Power to the magnetrons is supplied by an Advanced Energy® pulsed DC power supply, set at a pulse frequency of 200kHz and a rate of 1.6µs.

SMA coatings with a thickness of 3 micrometers, measured with a Dectac, are produced. The compositions of the coatings are measured using energy dispersive X-ray spectroscopy, and the crystallinity of the coatings is conducted using XRD equipped with a Cu source.

Two sets of coatings are produced; one set is used for scratch testing, while the other set are removed from the silicon substrate leaving freestanding films, which are required for DSC analysis.

A Setaram Setsys Evolution 16/18 DSC, equipped with Setsoft 2000 software, is employed to evaluate the phase transformation temperatures of the intermetallic coatings. The thin films are annealed using the DSC at 1100$^{o}$C, then 550$^{o}$C at 5$^{o}$C/min heating and cooling rates.

Mechanical indentation of the coatings is undertaken in order to investigate their recovery properties. A Teer Coatings scratch tester equipped with a 5mm spherical tip is used to load the coatings, with loads increasing from 1 to 5 N. All mechanical indentation studies are undertaken at room temperature.

## 3.0 Results and discussion

*3.1 The NiTi target*

An off-cut from a NiTi target material evoked a DSC response when it was annealed in the DSC to 1100$^{o}$C for 1 hour followed by 550$^{o}$C for 5 hours. Similarly, the coatings showed a DSC response when they underwent the same heating cycle as the off-cut. Lower temperature anneals were not successful in producing a DSC response and thus it was decided that all coatings would undergo a high-temperature, 1100$^{o}$C anneal, followed by a low-temperature, 500$^{o}$C anneal.

The off-cut piece of the target material was heated to 1100$^{o}$C for 1 hour followed by 550$^{o}$C for 5 hours in a DSC and then cycled from 20 to 200$^{o}$C. Clear austenite peak, $A_p$, and martensite peak, $M_p$, phases were present at 100 and 60$^{o}$C, respectively, with corresponding phase transformation enthalpies of 12.5 and -7.2 J/g for $A_p$ and $M_p$, suggesting that the target material has the *potential* to produce coatings with SMA characteristics. Additional DSC cycling from 20 to 200$^{o}$C was undertaken and the results are summarised in table I. The first cycle of the thermal response from a NiTi off-cut is shown in figure 1.

*3.2 NiTi and NiTiHf compositions by sputter deposition*

The difference in the sputtering yields of the Ni and the Ti, [21] from the NiTi alloy target resulted in coatings that were approximately 5 at% Ti deficient. This Ti deficiency from the nominally supplied target has been reported by other studies [7]. Compensation for the loss of Ti usually takes place by either placing pure Ti discs on the surface of the sputter target [7] or by co-sputtering [12]. If the Ti depletion is not compensated for during growth, studies have found that Ti deficiency results in phase transformation temperatures below room temperature [14]. Thus, in this work co-sputtering NiTi with Ti compensated for Ti depletion. Varying the power to the Ti target controlled the composition of the coating produced, and Ti compositions

ranging from 45 to 65 at% Ti were deposited. Table II summarises the coatings deposited in this study by co-sputtering NiTi with Ti.

During the fabrication of the NiTiHf coatings, circular (1cm diameter) pure Ti discs were placed in the erosion track of the NiTi target to control the film stoichiometry and to compensate for the loss of Ti, and was co-sputtered with Hf. By varying the power to the Hf target, compositions of Hf ranging from 2 to 30 at% Hf were deposited. Table III shows the results from the experiments conducted by co-sputtering NiTi with Hf.

*3.3 XRD analysis*

Figure 2 shows the XRD spectra of the NiTi films, over a 2θ of 35 to 60$^{o}$, before and after annealing. The films are not heated during deposition and the as-deposited films show a broad XRD peak with no texturing, suggesting an amorphous structure [22]. Heat treatment of the film at 1100$^{o}$C for 1 hour followed by a low temperature 550$^{o}$C for 5 hours is sufficient to crystallise the film and results in two major phases becoming present at room temperature. The first major peak at a 2θ of 41$^{o}$ is the monoclinic –(111) peak due to martensite [14]. The other major 2θ peak at 43$^{o}$ is the martensite B19’ (020) reflection [14,22,23]. The martensite (012) reflection is present at a 2θ of 44$^{o}$ [23]. It is to be expected that the martensite phase be dominant at room temperature and only diminish as the sample is heated. At higher temperatures, the austenite (110) cubic phase dominates at a 2θ of 42$^{o}$. In fact, studies by Uchil et al. [23] and Pattabi et al, [24] have followed the evolution of the austenite (110) phase by utilising a heated stage fitted to their XRD instrument. Uchil et al, [23] have interrogated the area under the austenite (110) peak as a means to elucidate the phase transformation and have concluded that this method is far more sensitive in measuring smaller volume fractions that undergo phase transformations, than that determined by

routine thermal DSC analysis. Unfortunately, it was not possible to access in this study and thus only room temperature XRD data and DSC analysis could be used for phase transformation behaviour. Further analysis of the XRD spectra was undertaken to determine the presence of precipitates formed by excess nickel or titanium. The XRD spectrum of the annealed NiTi film in figure 2 shows a number of peaks between 42 and 46$^{o}$ suggesting the presence of nickel rich precipitates. Excess nickel, for example, forms $Ni_3Ti$ [25], $Ni_3Ti_2$ [25] and/or $Ni_4Ti_3$ [14,14] at high temperatures, and the associated XRD peaks are to be found at approximate 2θ values of 39$^{o}$, 43$^{o}$, 47$^{o}$, 52$^{o}$ and 73$^{o}$ [25]. Excess titanium shows the presence of a (115) reflection due to $Ti_2Ni$ at a 2θ of approximately 41$^{o}$, and this could be present in the shoulder of our –(111) peak. As these peaks are relatively small compared with our martensite and austenite peaks, it is thought that the combination of pulse DC sputtering and our high temperature 1100$^{o}$C anneals used are sufficient to disperse these precipitates. XRD peaks associated with excess titanium forming $TiO_2$ in either an anatase or rutile phase [26]was within the background noise of our XRD spectrum and therefore need not be discussed further.

Figure 3 shows the XRD spectrum for the as-deposited NiTiHf thin film, showing a broad, low intensity XRD pattern at room temperature, indicating an amorphous structure. After annealing, peaks relating to the martensite -(111) and (101) appear. However, additional martensite peaks of (022), (020), (110) and (011) as identified by Tong et al., [9] are not present in these films. These differences could be associated with the processing involved as Tong et al., [9] employed rapid thermal annealing for 25 s as an alternative route to crystallise their NiTiHf films.

*3.4 DSC analysis*

For the phase transformation studies, the NiTi and the NiTiHf films were peeled from the silicon substrates so as to obtain phase transformation measurements without any stress [14]. Both the NiTi and NiTiHf samples were heated at a rate of 10$^{o}$C/min using the DSC. The samples, in the case of the NiTi films were cycled from 20 to 200$^{o}$C and 20 to 500$^{o}$C for the NiTiHf films, in order to determine the phase transformation characteristics.

*3.4.1The NiTi films*

Figure 4 shows the first heating and cooling cycle of the NiTi film containing 52 at% Ti. An additional 3 cycles was performed on this sample to verify reproducibility and the results of the phase transformations and the resulting enthalpies are shown in table IV. From the first cycle, we see that the peak of the phase transformation occurs at 107$^{o}$C and 68$^{o}$C for the austenite and martensite phase transformations, respectively. This hysteresis of 40$^{o}$C in the thin films reflects the hysteresis observed for the target material. For subsequent cycles in the NiTi film, the hysteresis falls to approximately 35$^{o}$C, again reflecting the characteristics of the target. The enthalpies for both the austenite and martensite phase transformations are higher in relative values when compared with the enthalpies calculated for the NiTi target material. The higher enthalpy values in the films indicate a greater portion of the film underwent a phase transformation than it did in the target material, another effect of the film being denser due to pulse DC sputtering and having fewer defects. A study by Botterill et al, [27] shows a similar temperature hysteresis for their NiTi films containing 52.5 at% Ti.

The NiTi film containing 65 at% Ti also underwent cyclic testing in the DSC from 20 to 200$^{o}$C. From the results, which are summarised in table V, the first cycle shows a phase transformation at 103$^{o}$C and 66$^{o}$C for the austenite and martensite phases,

respectively. The hysteresis is around 40$^{o}$C, but the only difference between this film and the film containing 52 at% Ti is the difference in phase transformation enthalpies. They are smaller in value than the film containing 52 at% Ti and they are smaller in value than for the NiTi target. Thus, this seems to suggest that although NiTi shows SMA characteristics at 65 at% Ti, less of the material undergoes phase transformation than NiTi containing 52 at% Ti. This high saturation of the Ti in the NiTi matrix results in the excess Ti forming $Ti_2Ni$ [28] precipitates congregating at columnar-grain interface, impeding phase transformations, and thus offering some explanation of the low phase transformation enthalpies in this film compared with the target.

*3.4.2 NiTiHf*

A summary of the results associated with the NiTiHf thin films can be found in table VI. Samples with IDs L15 and N15, with compositions of 2 and 10 at% Hf, respectively, showed no phase transformations above room temperature.

Studies by Sanjabi et al, [12] and Grummon et al, [7] show that initial doping with Hf less than 5 at% lowers martensite start temperatures ($M_S$), to below 20$^{o}$C. The DSC used for this study does not have a cold-stage and thus cannot measure temperatures below 20$^{o}$C. For sample N15 whose composition was above 5 at% Ti, according to established results, we should expect to see a phase transformation above 20$^{o}$C. The Hf occupies the Ti site via direct substitution of the Ti atoms [7] and looking at the $Ti_{(50-X)}Hf_X$ composition portion of N15, we note that the sum of these are below the 50 at% Ti threshold required to observe phase transformations above room temperature [14].

With Hf additions greater than 20 at%, experimental results show that transformation temperatures increase significantly above 300$^{o}$C [12]. In this study, the NiTiHf coating with 30 at% Hf shows a two-stage austenite phase transformation upon

heating and a single martensite phase transformation upon cooling. The additional transformation in the austenite phase has been termed the 'R' phase and is an intermediate rhombohedral phase between the martensitic B19' phase and the austenitic B2 phase [12]. Other studies have also shown that films containing Hf greater than 16 at%, display this intermediate 'R' phase [7]. Basically the 'R' phase occurs because of the build up of internal stresses and the depletion of Ni in the matrix. TEM studies have shown that the R-phase transformation seems to nucleate around precipitates of $Ti_3Ni_4$ and provide a lower energy alternative to the martensite phase transformation [29]. The driving force behind multiple stage transformation behaviour have been proposed [30-32]however the most widely accepted view now is that the precipitates are distributed inhomogeneously [31], resulting is localised phase transformations separate from the rest of the matrix. Thus, the phase transformation does not occur and propagate through the entire material, but occurs in localised portions of the material, resulting in multiple transformation peaks [30,31].

Further, the transformation temperature in the coating with 30 at% Hf is around 150$^{o}$C, well below the transformation temperature that would be predicted using the results from Sanjabi et al, [12] for a similar composition of coating. The reason for such a large discrepancy is the difference in stoichiometry between the two studies; Sanjabi's coatings were stoichiometric NiTiHf, whereas the coating with 30 at% Hf deposited in this study was off-stoichiometry. This shows the versatility of the NiTiHf 'process window' over which NiTiHf can be compositionally engineered for a particular application at the expense of its phase transformation temperature.

Sanjabi et al, [12] showed that in the case of NiTiHf coatings, the annealing temperature was a function of Hf composition, requiring a crystallisation temperature of around 500$^{o}$C. In this study it was found that this temperature did not produce any

visible phase transformation in the coating. Much higher temperatures were required. The reason for this discrepancy is not clear at this moment, the differences between the two studies were that Sanjabi et al [12] used DC sputtering, whereas this study used the higher energy pulsed DC process. Furthermore, Sanjabi's coatings were near stoichiometric whereas the coatings produced in this study were off-stoichiometric (Ti and Hf) rich. Further work using rapid thermal annealing (RTA) is currently underway as an alternative route to crystallise the coatings.

*3.5 Mechanical Testing*

Both the NiTi and the NiTiHf films were mechanically tested for their recovery properties using scratch testing with a ball indenter at loads ranging from 1 to 5N. The vertical displacements were measured and the resulting, 'final' displacement calculated. The difference between the vertical displacements caused by the initial indentation compared with the vertical displacement when the load was removed was termed the permanent 'deformation' of the material.

A typical plot of the vertical displacement of a SMA coating versus the load applied is shown in figure 5. The deformation of both the NiTi and NiTiHf coatings fabricated in this study are summarised in table VII. For the coating containing 52 at% Ti, a load of 1N results a vertical displacement of 7.5μm and increasing the load to a maximum of 5N results in a vertical displacement of 17μm. When the load is removed from the sample, the coating recovers to a degree, which results in a permanent deformation of 10.5μm. We see that as the Ti content is increased to 65 at% Ti, the deformation increases to 30μm, 3 times larger than the film containing 52 at% Ti. Similarly for the Hf-containing films, we observe that increasing Hf content in the film results in an almost doubling of the film deformation.

## *4.0 Conclusions*

- Pulse DC sputtering has been employed to fabricate NiTi and NiTiHf coatings onto silicon substrates. As deposited coatings are amorphous. Coating compositions of NiTi containing 45 to 65 at% can be crystallised by a thermal treatment. Removing the coatings from the silicon substrates and heating the films in a DSC at a temperature of 1100$^{o}$C for 1 hour followed by 550$^{o}$C for 5 hours, results in crystallisation. XRD reveals –(111) and (020) martensite peaks at room temperature.
- In the NiTi thin films, the endothermic austenite peak phase transformation occurs at around 105$^{o}$C and the exothermic peak martensite phase transformation occurs at 65$^{o}$C, a hysteresis of 40$^{o}$C. Phase transformation enthalpies of the NiTi containing 52 at% Ti were similar to those obtained for the NiTi source material used to fabricate the coatings by pulsed DC sputtering. For the NiTi films containing 65 at% Ti phase transformation enthalpies were lower than those of the sputtering target, however, the hysteresis remained unchanged at 40$^{o}$C. This is understood to be due to excess Ti forming $Ti_2Ni$ precipitates within the 'as deposited' then heat-treated films. Thus, although the stoichiometric 'process window' to produce a phase transformation in NiTi SMAs is quite large, there is a trade-off in transformation enthalpy, ie the *amount* of material that undergoes an austenite or martensite transformation, with transformation temperature.
- Co-sputtering NiTi with Hf and varying the power to the Hf target from 15 to 70W, NiTiHf films with Hf compositions ranging from 2 to 30 at% Hf have been fabricated. XRD reveals an amorphous as-grown film, which requires a

1100$^{o}$C anneal for 1 hour to crystallise the film. XRD reveals martensitic - (111) and (020) planes after this heat treatment.

- NiTiHf coatings with Hf contents of 2 and 10 at% show no visible phase transformation above 20$^{o}$C.
- DSC of the films containing 30 at% Hf has shown a 'R' phase transition, which occurs between the room temperature B19' phase and the high temperature B2 phase. It is understood that this phase is present in films that have high internal stresses and nucleate near $Ti_3Ni_4$ precipitates. Such precipitates provide a low energy alternative by providing sites for nucleation. Precipitates are distributed randomly throughout the matrix and therefore transformations occur at distinct locations resulting in multiple peaks.
- Measurements of the recovery properties of the films using a scratch tester with a spherical indenter at loads ranging from 1 to 5N at room temperature show that films containing 65 at% Ti are able to deform 3 times more than films containing 52 at% Ti. For the films containing Hf, increasing the Hf composition from 2 at% to 30 at%, doubled the deformation measured in the films.

**References**

1 P. Pappas, D. Bollas, J. Parthenios, V. Dracopoulos, and C. Galiotis, Smart Mater Struct 16, 6 (2007).

2 Y. Bellouard, Mater. Sci. Eng. A 481-482, 1-2 C (2008).

3 J. Jayender, R. V. Patel, S. Nikumb, and M. Ostojic, IEEE Trans Control Syst Technol 16, 2 (2008).

4 M. Leester-Schaf̈del, B. Hoxhold, C. Lesche, S. Demming, and S. Buttgenbach, Microsyst Technol 14, 4-5 (2008).

5 J. Otubo, O. D. Rigo, A. A. Coelho, C. M. Neto, and P. R. Mei, Mater. Sci. Eng. A 481-482, 1-2 C (2008).

6 A. S. Paula, K. K. Mahesh, and F. M. Braz Fernandes, Eur. Phys. J. : Spec. Top. 158, 1 (2008).

7 D. S. Grummon, JOM 55, 12 (2003).

8 R. G. Wellman, and J. R. Nicholls, Tribol Int 41, 7 (2008).

9 Y. Tong, Y. Liu, J. Miao, and L. Zhao, Scripta Mater. 52, 10 (2005).

10 G. S. Bigelow, S. A. Padula II, A. Garg, and R. D. Noebe, Correlation between Mechanical Behavior and Actuator-Type Performance of Ni-Ti-Pd High-Temperature Shape Memory Alloys, San Diego, CA ed. 2007).

11 S. Padula II, R. Noebe, G. Bigelow, D. Culley, M. Stevens, N. Penney, D. Gaydosh, T. Quackenbush, and B. Carpenter, Development of a HTSMA-Actuated Surge Control Rod for High-Temperature Turbomachinery Applications, Waikiki, HI ed. 2007), p. 5862.

12 S. Sanjabi, Y. Z. Cao, and Z. H. Barber, Sens & Act A: Physical 121, 2 (2005).

13 Y. Tong, Y. Liu, and J. Miao, Thin Solid Films 516, 16 (2008).

14 E. Wibowo, and C. Y. Kwok, J Micromech Microengineering 16, 1 (2006).

15 M. Čada, J. W. Bradley, G. C. B. Clarke, and P. J. Kelly, J Appl Phys 102, 6 (2007).

16 S. K. Karkari, A. R. Ellingboe, C. Gaman, I. Swindells, and J. W. Bradley, J Appl Phys 102, 6 (2007).

17 K. Sarakinos, J. Alami, and M. Wuttig, J Phys D 40, 7 (2007).

18 C. P. Frick, T. W. Lang, K. Spark, and K. Gall, Act. Mater. 54, 8 (2006).

19 www.teercoatings.co.uk

20 www.pikem.com

21 V. Abhilash, M. A. Sumesh, and S. Mohan, Smart Mater Struct 14, 5 (2005).

22 E. Wibowo, and C. Y. Kwok, J Micromech Microengineering 16, 1 (2006).

23 S. Miyazaki, and A. Ishida, Mat. Sci & Eng A 273-275, (1999/12/15).

24 J. Uchil, F. M. B. Fernandes, and K. K. Mahesh, Mater Charact 58, 3 (2007).

25 M. Pattabi, K. Ramakrishna, and K. K. Mahesh, Mater. Sci. Eng. A 448, 1-2 (2007).

26 Y. W. Gu, B. Y. Tay, C. S. Lim, and M. S. Yong, App. Surf. Sci. 252, 5 (2005).

27 S. Boukrouh, R. Bensaha, S. Bourgeois, E. Finot, and M. C. Marco de Lucas, Thin Solid Films 516, 18 (2008).

28 N. W. Botterill, and D. M. Grant, Mater. Sci. Eng. A 378, 1-2 SPEC. ISS. (2004).

29 H. Cho, H. Y. Kim, and S. Miyazaki, Mat. Sci. and Eng: A 438-440, (2006).

30 M. C. Carroll, C. Somsen, and G. Eggeler, Scrip. Mater. 50, 2 (2004).

31 A. Dlouhý, J. Khalil-Allafi, and G. Eggeler, Z Metallkd 95, 6 (2004).

32 J. K. Allafi, A. Dlouhy, K. Neuking, and G. Eggeler, Influence of Precipitation and Dislocation Substructure on Phase Transformation Temperatures in a Ni-Rich NiTi-Shape Memory Alloy, Villa Olmo, Como ed. 2001).

**Table I:** Summary of the phase transformation temperatures for 3 cycles of 20 to 200°C measured in a small piece of the NiTi target material.

| **Heating Cycle** | | | |
|---|---|---|---|
| **Cycle** | **1** | **2** | **3** |
| $A_S$ (°C) | 98 | 73 | 92 |
| $A_P$ (°C) | 105 | 103 | 101 |
| Enthalpy (J/g) | 12.5 | 12 | 11.5 |
| **Cooling cycle** | | | |
| **Cycle** | **1** | **2** | **3** |
| $M_S$ (°C) | 73 | 71 | 69 |
| $M_P$ (°C) | 66 | 67 | 64 |
| Enthalpy (J/g) | -7.2 | -7.3 | -4.4 |

**Table II:** Summary of the experiments conducted by co-sputtering NiTi with Ti. Varying power to the Ti target controlled film stoichiometry. All experiments were conducted in Ar at a pressure of 10 mTorr.

| Sample ID | Composition (at%) | | Power (W) | |
|---|---|---|---|---|
| | Ni | Ti | NiTi | Ti |
| D40 | 55 | 45 | 400 | 0 |
| E15 | 53 | 47 | 150 | 50 |
| H25 | 48 | 52 | 150 | 100 |
| I25 | 48 | 52 | 150 | 80 |
| J25 | 48 | 52 | 150 | 100 |
| K25 | 35 | 65 | 150 | 120 |

**Table III:** Summary of the experiments conducted by pulse-DC co-sputtering NiTi with Hf. Film stoichiometry was controlled by varying power to the Hf target. All experiments were conducted in Ar at a pressure of 10 mTorr.

| Sample ID | Composition (at%) | | | Power (W) | |
|---|---|---|---|---|---|
| | Ni | Ti | Hf | NiTi | Hf |
| L15 | 50 | 48 | 2 | 150 | 10 |
| N15 | 50 | 38 | 10 | 150 | 15 |
| K15 | 40 | 30 | 30 | 150 | 70 |

**Table IV.** The calculated DSC response obtained from a NiTi coating containing 52 at% Ti. The coating was cycled from 20 to 200°C and each time, the DSC software used to calculate the enthalpies.

| **Heating Cycle** | | | | |
|---|---|---|---|---|
| **Cycle** | **1** | **2** | **3** | **4** |
| $A_S$ (°C) | 94 | 93 | 90 | 90 |
| $A_P$ (°C) | 107 | 101 | 100 | 98 |
| $A_F$ (°C) | 115 | 112 | 112 | 108 |
| Enthalpy (J/g) | 13.9 | 13.4 | 16.7 | 13.0 |
| **Cooling cycle** | | | | |
| **Cycle** | **1** | **2** | **3** | **4** |
| $M_S$ (°C) | 74 | 72 | 69 | 69 |
| $M_P$ (°C) | 68 | 66 | 64 | 63 |
| $M_F$ (°C) | 65 | 61 | 59 | 59 |
| Enthalpy (J/g) | -9.5 | -9.9 | -11.1 | -9.5 |

**Table V.** The DSC results obtained from the NiTi film containing 65 at % Ti. The coating is off stoichiometric, with excess Ti that forms $Ti_2Ni$ precipitates and results in reduced phase transformation enthalpies to a stoichiometric NiTi coating.

| **Heating Cycle** | | |
|---|---|---|
| **Cycle** | **1** | **2** |
| $A_S$ ($^oC$) | 93 | 91 |
| $A_P$ ($^oC$) | 103 | 98 |
| $A_F$ ($^oC$) | 112 | 110 |
| Enthalpy (J/g) | 5.8 | 11 |
| **Cooling cycle** | | |
| **Cycle** | **1** | **2** |
| $M_S$ ($^oC$) | 70 | 67 |
| $M_P$ ($^oC$) | 66 | 63 |
| $M_F$ ($^oC$) | 61 | 59 |
| Enthalpy (J/g) | -6.4 | -4.7 |

**Table VI.** The calculated responses from the DSC obtained from the NiTiHf coating containing 30 at% Hf. We observe a 2-stage phase transformation on the heating cycle and only a single-phase transformation phase during the cool-down cycle.

| **Heating Cycle** | | |
|---|---|---|
| | **Stage** | |
| **Cycle 1** | **1st** | **2nd** |
| $A_S$ ($^oC$) | 98 | 149 |
| $A_P$ ($^oC$) | 103 | 153 |
| $A_F$ ($^oC$) | 109 | 160 |
| Enthalpy (J/g) | 2.23 | 3.64 |
| **Cooling cycle** | | |
| | **Stage** | |
| **Cycle** | **1st** | **2nd** |
| $M_S$ ($^oC$) | 99 | - |
| $M_P$ ($^oC$) | 97 | - |
| $M_F$ ($^oC$) | 90 | - |
| Enthalpy (J/g) | -7.2 | - |

**Table VII.** Summary of the results using loads of 1 to 5N to deform the NiTi and NiTiHf films. The deformation in the films is strongly dependant upon the film composition.

| | | | Displacement | |
|---|---|---|---|---|
| **Sample** | **Deformation (µm)** | **Material composition** | **Start (µm)** | **Final (µm)** |
| K15 | 30 | 65 at% Ti | 2 | 32 |
| J25 | 10.5 | 52 at% Ti | 7.5 | 17 |
| O15 | 13 | 30 at% Hf | 12 | 25 |
| L15 | 7 | 2 at% Hf | 0 | 7 |

## List of figures

**Figure 1:** The DSC response from the NiTi target used to sputter the coatings in this study. Clear austenite and martensite phase transitions are visible. The target is calculated to have a hysteresis of 40$^{o}$C.

**Figure 2.** Typical room temperature XRD spectra obtained from the NiTi coatings. Before crystallisation the coatings are amorphous and after annealing the coatings are pre-dominantly martensitic. Additional peaks between 2θ of 41$^{o}$ and 46$^{o}$ could be due to precipitate formation.

**Figure 3.** Room temperature XRD spectra obtained from the NiTiHf coating containing 30 at% Hf, before and after annealing.

**Figure 4.** The first thermal cycle response obtained from a NiTi film containing 52 at% Ti. The peak of the austenite phase transformation occurs at 105$^{o}$C and the peak of the martensite phase transformation occurs at 65$^{o}$C. The hysteresis of the sample is calculated to be around 40$^{o}$C – similar to that of the target. For subsequent cycles, the hysteresis falls to 35$^{o}$C, remaining constant for the next three cycles.

**Figure 5.** A typical vertical displacement versus load curve obtained from the NiTi and NiTiHf coatings, at room temperature. As the load increases from 1 to 5N, the displacement of the film increases. As the load reduces from 5 to 1 N, the film recovers, but a 'permanent displacement', termed in this study as 'deformation,' in the coatings occurs. It is this calculated deformation that is reported in table VII.

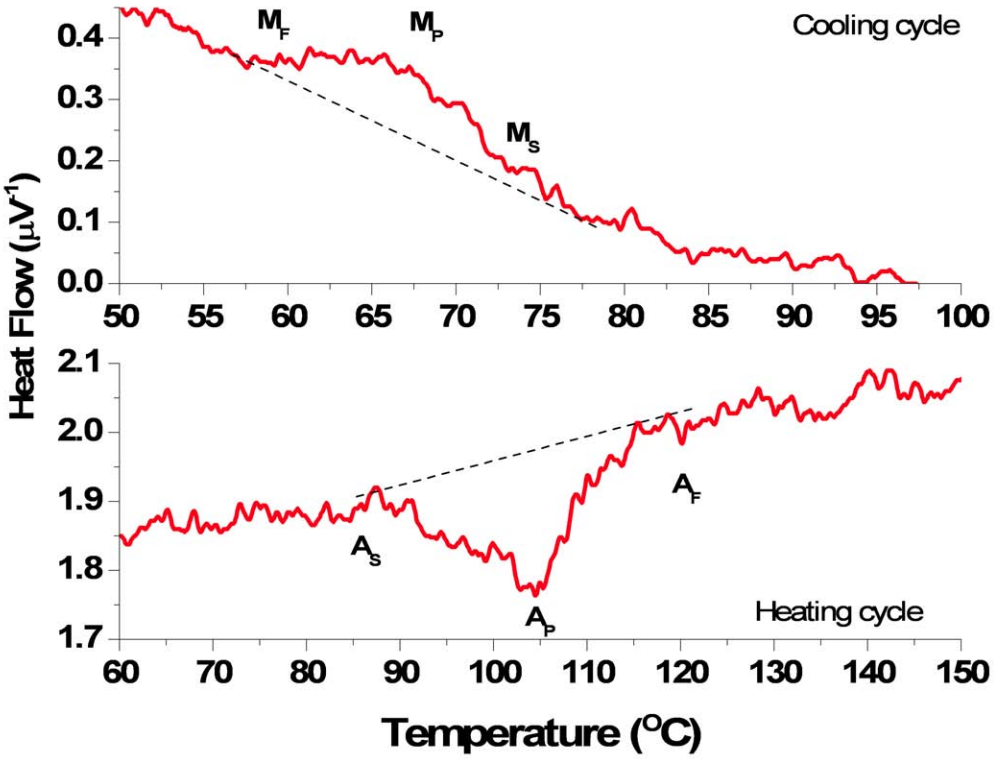


**Figure 1.**

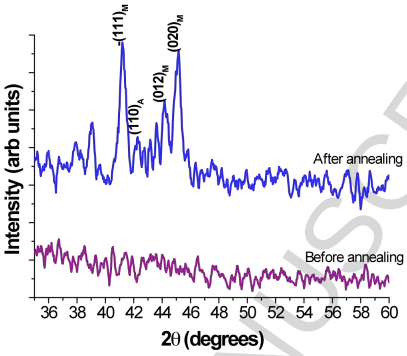

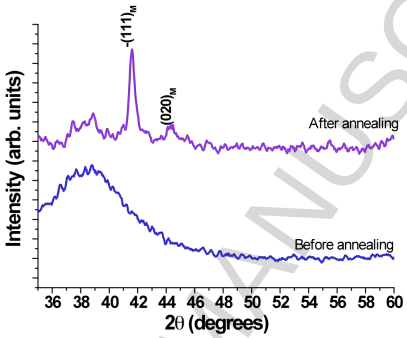

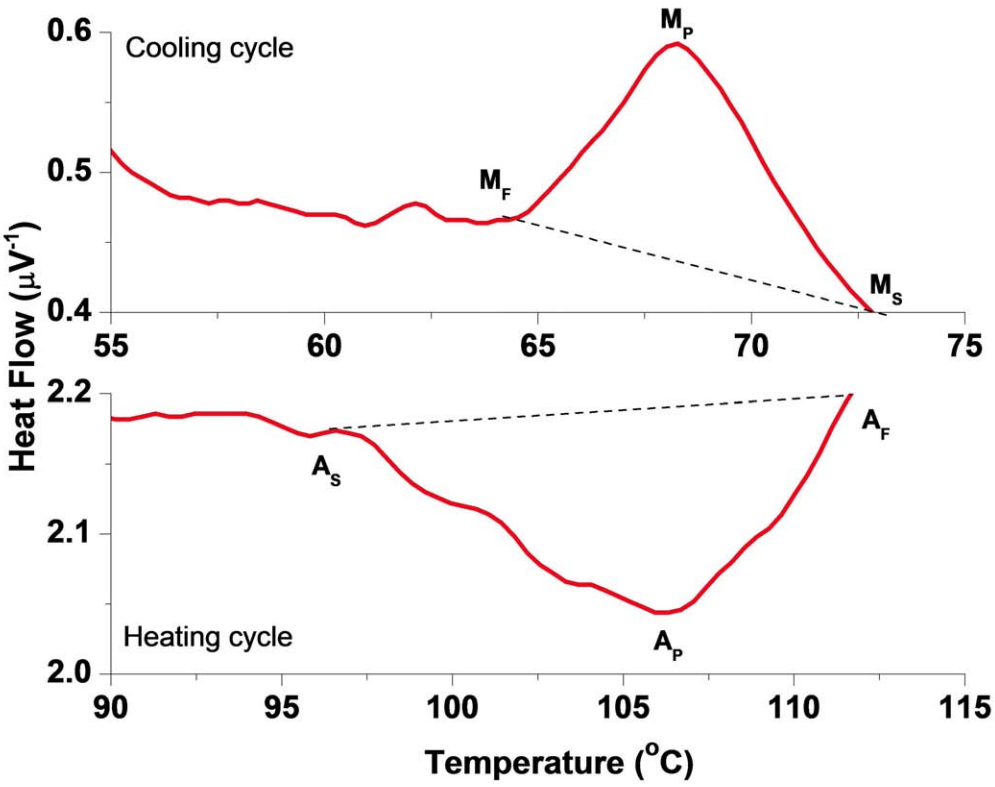


**Figure 4.**

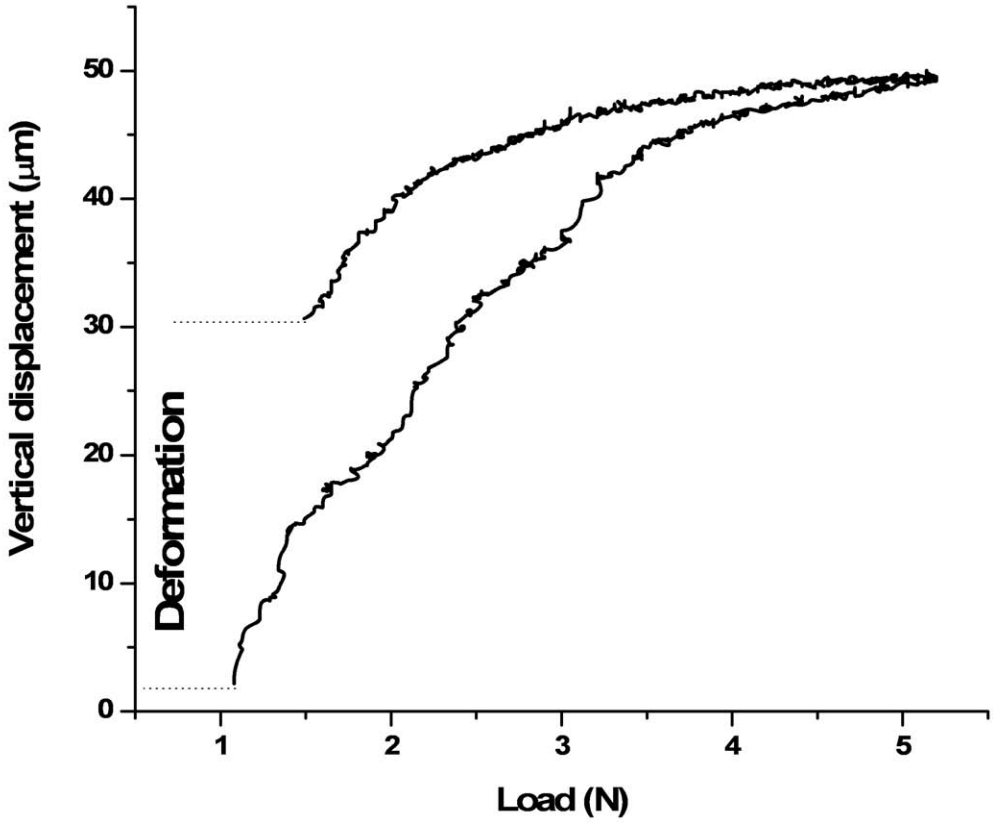


**Figure 5.**

# Nickel titanium and nickel titanium hafnium shape memory alloy thin films

Rao, Jeff

2010-04-01T00:00:00Z

J. Rao, T. Roberts, K. Lawson, J. Nicholls, Nickel titanium and nickel titanium hafnium shape memory alloy thin films, Surface and Coatings Technology, Volume 204, Issue 15, 25 April 2010, Pages 2331-2336

http://dx.doi.org/10.1016/j.surfcoat.2009.12.025